

Manuscript Number: HAZMAT-D-20-00519R1

Title: Potential syntrophic associations in anaerobic Naphthenic Acids biodegrading consortia inferred with microbial interactome networks

Article Type: Research Paper

Keywords: Anaerobic microcosms; Indigenous microorganisms; Interactome network; Microbial function; Electron acceptor

Corresponding Author: Professor Bin Ma,

Corresponding Author's Institution:

First Author: Xiaofei Lv

Order of Authors: Xiaofei Lv; Bin Ma; Korris Lee; Ania Ulrich

Abstract: Naphthenic acids (NAs) can be syntrophically metabolized by indigenous microbial communities in pristine sediments beneath oil sands tailings ponds. Syntrophy is an essential determinant of the microbial interactome, however, the interactome network in anaerobic NAs-degrading consortia has not been previously addressed due to complexity and resistance of NAs. To evaluate the impact of electron acceptors on topology of interactome networks, we inferred two microbial interactome networks for anaerobic NAs-degrading consortia under nitrate- and sulfate-reducing conditions. The complexity of the network was higher under sulfate-reducing conditions than nitrate-reducing conditions. Differences in the taxonomic composition between the two modules implies that different potential syntrophic interactions exist in each network. We inferred the presence of the same syntrophic microorganisms, from genera *Bellilinea*, *Longilinea*, and *Litorilinea*, initiating the metabolism in both networks, but within each network, we predicted unique syntrophic associations that have not been reported. Electron acceptor has a large effect on the interactome networks for anaerobic NAs-degrading consortia, offers insight into an unrecognized dimension of these consortia. These results provide a novel approach for exploring potential syntrophic relationships in biodegrading processes to help cost-effectively remove NAs in oil sands tailings ponds.

### **Novelty Statement**

Syntrophic processes make essential contribution in anaerobic biodegradation of NAs from sediments of oil sands tailings ponds (OSTP). This study inferred two microbial interactome networks for anaerobic NA-degrading consortia enriched from sediments of OSTP under nitrate- and sulfate-reducing conditions, respectively. Specifically, within each network, unique syntrophic associations were predicted that have not been reported previously. Our results demonstrate that electron acceptor has a large effect on the microbial interactome networks for anaerobic NA-degrading consortia, offer vital insight into an unrecognized dimension of these consortia, and provide a novel approach for exploring potential syntrophic relationships.

## Highlights

- Inferred microbial interactome networks in anaerobic NA-degrading consortia
- Sulfate-reducing networks were more complexity than nitrate-reducing networks
  - Differences between microbial networks can be ascribed to electron acceptors
  - Predicted potential syntrophic associations in anaerobic NA-degrading consortia



## ABSTRACT

Naphthenic acids (NAs) can be syntrophically metabolized by indigenous microbial communities in pristine sediments beneath oil sands tailings ponds. Syntrophy is an essential determinant of the microbial interactome, however, the interactome network in anaerobic NAs-degrading consortia has not been previously addressed due to complexity and resistance of NAs. To evaluate the impact of electron acceptors on topology of interactome networks, we inferred two microbial interactome networks for anaerobic NAs-degrading consortia under nitrate- and sulfate-reducing conditions. The complexity of the network was higher under sulfate-reducing conditions than nitrate-reducing conditions. Differences in the taxonomic composition between the two modules implies that different potential syntrophic interactions exist in each network. We inferred the presence of the same syntrophic microorganisms, from genera *Bellilinea*, *Longilinea*, and *Litorilinea*, initiating the metabolism in both networks, but within each network, we predicted unique syntrophic associations that have not been reported. Electron acceptor has a large effect on the interactome networks for anaerobic NAs-degrading consortia, offers insight into an unrecognized dimension of these consortia. These results provide a novel approach for exploring potential syntrophic relationships in biodegrading processes to help cost-effectively remove NAs in oil sands tailings ponds.

1            Potential Syntrophic Associations in Anaerobic Naphthenic Acids  
2            Biodegrading Consortia Inferred with Microbial Interactome Networks

3                            Xiaofei Lv<sup>1</sup>, Bin Ma<sup>2\*</sup>, Korris Lee<sup>3</sup>, Ania Ulrich<sup>3</sup>

4            1. Department of Environmental Engineering, China Jiliang University, Hangzhou  
5            310018, China

6            2. Institute of Soil and Water Resources and Environmental Science, College of  
7            Environmental and Resource Sciences, Zhejiang University, Hangzhou, 310058, China

8            3. Department of Civil and Environmental Engineering, University of Alberta,  
9            Edmonton, Alberta, T6G 2W2, Canada

10

11            \*Corresponding authors:

12            Bin Ma, email bma@zju.edu.cn

13 **ABSTRACT**

14 Naphthenic acids (NAs) can be syntrophically metabolized by indigenous microbial  
15 communities in pristine sediments beneath oil sands tailings ponds. Syntrophy is an essential  
16 determinant of the microbial interactome, however, the interactome network in anaerobic NAs-  
17 degrading consortia has not been previously addressed due to complexity and resistance of NAs.  
18 To evaluate the impact of electron acceptors on topology of interactome networks, we inferred  
19 two microbial interactome networks for anaerobic NAs-degrading consortia under nitrate- and  
20 sulfate-reducing conditions. The complexity of the network was higher under sulfate-reducing  
21 conditions than nitrate-reducing conditions. Differences in the taxonomic composition between  
22 the two modules implies that different potential syntrophic interactions exist in each network.  
23 We inferred the presence of the same syntrophic microorganisms, from genera *Bellilinea*,  
24 *Longilinea*, and *Litorilinea*, initiating the metabolism in both networks, but within each network,  
25 we predicted unique syntrophic associations that have not been reported. Electron acceptor has a  
26 large effect on the interactome networks for anaerobic NAs-degrading consortia, offers insight  
27 into an unrecognized dimension of these consortia. These results provide a novel approach for  
28 exploring potential syntrophic relationships in biodegrading processes to help cost-effectively  
29 remove NAs in oil sands tailings ponds.

30 **Keywords:** Anaerobic microcosms; Indigenous microorganisms; Interactome network;  
31 Microbial function; Electron acceptor

32

## 33 1. Introduction

34 Naphthenic acids (NAs) are a complex mixture of carboxylic acids that occur naturally in  
35 petroleum [1]. NAs can cause engineering and production difficulties through corrosion of  
36 refinery plant and deposition as salts in pipelines [2]. NAs also cause environmental problems  
37 because of their toxicity, recalcitrance, and persistence. NAs may persist in the environment for  
38 many years, especially in aged wastewater. NAs concentrations in wastewaters can remained >  
39  $19\text{ mg L}^{-1}$  even after several decades [3]. NAs have been identified as the main component  
40 responsible for the acute toxicity in produced waters in the oil sands tailing ponds (OSTP) in  
41 northeastern Alberta, Canada [4]. The ponds are estimated to exceed a billion cubic meters by  
42 2025 and are already visible from space [5].

43 Bioremediation is an attractive option for reducing the toxicity of NAs wastes[6]. The  
44 anaerobic degradation of simple single-ringed surrogate NAs has been reported under sulfate-,  
45 nitrate-, and iron-reducing conditions [7,8] . Syntrophy is a beneficial metabolic process  
46 occurring between organisms, where a given compound can be only be degraded by one  
47 organism when a second organism consumes the intermediate products and keeps them at a low  
48 concentrations [9]. Syntrophic metabolism of hydrocarbons is common in methanogenic  
49 ecosystems where electron acceptors are limited or absent [10]. In syntrophic environments, the  
50 syntrophic organisms initially degrade hydrocarbons to intermediates such as acetate, formate, or  
51  $\text{H}_2$ . Methanogens consume the intermediates and keep them at low concentrations to make the  
52 initial anaerobic oxidation energetically favorable. However, it is hard to figure out syntrophic  
53 relationships in the communities without any reference information. The high proportion of  
54 microbial “dark matters”, the uncultured environmental microbes, also hinder discovering  
55 syntrophic relationships.



56 Genomic analysis have shown that syntrophic interactions are essential for anaerobic  
57 biodegradation of hydrocarbons [11], and a recent review comprehensively describes the  
58 underlying principles of syntrophic hydrocarbon degradation [9]: the initial fermentative  
59 organism degrades the hydrocarbons with reactions that are not thermodynamically favorable,  
60 and produces intermediates such as acetate, formate, and/or H<sub>2</sub> that are consumed by  
61 methanogens [9]. Recent studies have also shown that benzene is syntrophically degraded in the  
62 presence of electron acceptors such as nitrate [12], ferric iron [13], and sulfate [14]. For example,  
63 methane from gas hydrates in ocean sediments is consumed by anaerobic methane-oxidizing  
64 archaea that associate with sulfate-reducing Deltaproteobacteria [15]. Hermann et al.[16] found  
65 that *Cryptanaerobacter* degraded benzene into intermediates such as acetate/H<sub>2</sub>, which were then  
66 consumed by sulfate reducers. van der Zaan et al.[12] used stable isotope probing (SIP) with  
67 <sup>13</sup>C<sub>6</sub>-benzene to identify that the Peptococcaceae degraded benzene to H<sub>2</sub>/acetate that was then  
68 consumed by the Betaproteobacteria, with both processes coupled to the nitrate reduction.  
69 Syntrophy also occurs in methanogenic cultures which can degrade surrogate NAs [7] . Since  
70 degradation of complex organics is generally more efficient under nitrate- and sulfate-reducing  
71 conditions, understanding the syntrophic interactions under nitrate- and sulfate-reducing  
72 conditions is critical for understanding anaerobic degradation of NAs.

73 The microbial interactome represents all of the interactions taking place among all  
74 community members. A recent study highlighted the critical role of microbial interactions in  
75 shaping microbial communities structure [18]. Interactome network inferred from abundance  
76 data can allow better understanding of community composition and function [19], and is a  
77 promising approach to explore microbial interactions in complex environments such as  
78 gastrointestinal tracts [20], bioreactors [21], soils [22,23], and oceans [19]. The complexity of

79 these networks provides a new perspective on the structure of the microbial communities and  
80 adds to our understanding of microbial ecology [24]. However, to the best of our knowledge, the  
81 microbial interactome network and potential syntrophic relationships in the anaerobic NAs-  
82 degradation processes has not been previously addressed due to extremely slow degradation  
83 rates.

84 This study inferred the microbial interactome networks for anaerobic NAs-degrading  
85 consortia enriched from sediments underlying OSTP under either nitrate- or sulfate-reducing  
86 conditions to: (i) determine if the electron acceptor affects the topological patterns of interactome  
87 networks and (ii) predict syntrophic interactions involved in anaerobic NAs-degradation.

## 88 **2. Materials and methods**

### 89 *2.1 Naphthenic acid substrates*

90 A stock solution of acid extracted organics (AEO) was prepared by extracting acidified  
91 (pH<2) oil sands processing-affected water (OSPW) with dichloromethane as previously  
92 described [25]. The Merichem NAs were NA mixtures obtained from Merichem Chemicals and  
93 Refinery Services LLC. (Houston, Texas).

### 94 *2.2 Microcosm establishment*

95 Sediments were collected from the Northwest edge of the Suncor Energy Inc.'s South  
96 Tailings Pond, situated approximately 35 km north of Fort McMurray, Alberta, Canada [26]. The  
97 clay and sand sediments were sampled from 6.1-6.4 m below ground surface (mbgs) and 37.7-  
98 38.7 mgbs, respectively [28]. Nitrate- and sulfate-reducing consortia were enriched from either  
99 clay or sand sediments amended with either acid extractable organics (AEO) or Merichem NAs  
100 (Merichem Chemicals and Refinery Services LLC.; Houston, Texas) [2]. A stock solution of

101 AEO was prepared by extracting acidified (pH<2) oil sands process-affected water with  
102 dichloromethane as previously described [27].

103 Microcosms were established from enrichments that were actively depleting NAs and  
104 electron acceptors. The microcosms consisted of 50 mL of original sediments inoculated into 450  
105 mL of groundwater from the same site. Electron acceptors (7 mmol L<sup>-1</sup> sodium nitrate or 14  
106 mmol L<sup>-1</sup> sodium sulfate) and NA substrates (100 mmol L<sup>-1</sup> Merichem NAs or 100 mmol L<sup>-1</sup>  
107 AEO NAs) were added individually to each incubation from sterile anoxic stock solutions using  
108 N<sub>2</sub>-flushed syringes. The nitrate and sulfate concentrations in all enrichments were monitored  
109 monthly and maintained at 7 and 14 mmol L<sup>-1</sup>, respectively. Each treatment was performed in  
110 triplicate. Autoclaved sterile controls were treated under 121 °C for 30 min for all experiments.  
111 The sterility was approved by both the methane production and DNA extraction. The procedural  
112 blanks for both physiochemical analysis and DNA extraction were performed during  
113 experiments.

### 114 *2.3 Microbial community assessment*

115 At 0, 163, and 331 days of incubation, representing different stages of microbial activities  
116 in the microcosms [28], we filtered the subsampled liquid with a 0.22 µm PVDF Millipore filter  
117 membrane for DNA extraction. The V3-V4 region of 16S rDNA was amplified and barcoded  
118 with primer set F515 and R806 [27], and sequenced using the Illumina MiSeq platform at the  
119 Molecular Biology Service Unit, University of Alberta. All samples generated a total of  
120 6,631,481 sequences. After removing low quality sequences (expected error threshold=1),  
121 singletons, and chimeras, we obtained 5,618,515 sequences and defined 1165 operational  
122 taxonomic units (OTUs) with cutoff of 97% similarity and assigned to taxa using the UPARSE

123 **pipeline.** The sequences were deposited in the sequence read archive (SRA) database with  
124 accession number SRR5690441.

#### 125 ***2.4 Interactome network inference***

126 Interactome networks were constructed based on a maximal information coefficient  
127 (MIC) calculated with the minerva package in R [29]. To reduce rare operational taxonomic  
128 units (OTUs) in the dataset, we removed OTUs with relative abundances less than 0.01%. The  
129 nodes in this network represent OTUs and environmental variables. We adjusted all  $p$ -values for  
130 multiple tests using the Benjamini and Hochberg FDR controlling procedure in the multtest  
131 package of R. The direct correlation dependencies were distinguished using the network  
132 deconvolution method [30]. The co-occurrence networks for clay and sand sediments were  
133 constructed separately based on MIC and FDR adjusted  $p$ -values. The MIC thresholds,  
134 determined by Random matrix theory (RMT) method [31], were 0.88 and 0.89 for nitrate and  
135 sulfate networks, respectively. Network properties were calculated with the igraph package in the  
136 R program [32].

#### 137 ***2.5 Module detection and keystone node identification***

138 We identified modules (group of nodes that are highly connected within the group with  
139 few connections outside the group) for nitrate- and sulfate-reducing networks using the greedy  
140 modularity optimization method (igraph: cluster\_fast\_greedy). The connectivity of each node  
141 was determined based on its within-module connectivity ( $K_{within}$ ) and among-module  
142 connectivity ( $K_{out}$ ; WGCNA: intramodularConnectivity). Node topologies were organized into  
143 four categories: network hubs, module hubs, articulation nodes, and peripherals. Subnetworks for  
144 each sample were generated based on the group of OTUs occurring in each sample. The network  
145 level topological properties were calculated with the igraph package.

## 146 **2.6 Statistical analysis**

147 All statistical analyses were conducted using R version 3.4.0 ([www.r-project.org](http://www.r-project.org)). The  
148 NAs-associated nodes in nitrate- and sulfate-reducing networks were identified using random  
149 forest models. Phylogenetic diversity was calculated with the phyloseq package. Pearson's  
150 correlations were used to determine the relationships between topological features of  
151 subnetworks and geochemical properties or phylogenetic diversity.

## 152 **3. Results**

### 153 **3.1 Interactome network topological characteristics**

154 To identify potential microbe-microbe interactions in anaerobic NAs-degrading  
155 consortia, we constructed interactome networks for the microbial succession in the nitrate- (Fig.  
156 1a) and sulfate-reducing (Fig. 1b) microcosms over 331 days of incubation. Both nitrate- and  
157 sulfate-reducing interactome networks exhibited non-random characteristics, as indicated by  
158 scale-free features (Fig. S1) and by comparison with the topological features of random networks  
159 generated using the same numbers of vertices and edges of both networks (Fig. S2a, b, Table 1).  
160 Both interactome networks had shorter diameters and mean path lengths, fewer neighbors, and  
161 larger transitivity than the corresponding random networks (Table 1). Network topological  
162 matrices (Table 1) and network associations across classes (Fig. 1c, d) showed that microbial  
163 association patterns were different in the nitrate- and sulfate-reducing networks. The link number  
164 in the nitrate-reducing network was larger than that in the sulfate-reducing network, but the giant  
165 subnetwork in the sulfate-reducing network was larger than that in the nitrate-reducing network  
166 (Fig. 1, Table 1). The nitrate-reducing network had longer diameter and mean path length, as  
167 well as smaller centrality than the sulfate-reducing network (Table 1). The associating patterns  
168 across dominant classes were different between the two networks (Fig. 1b, d). The numbers of

169 links associated with nodes assigned to Alphaproteobacteria and Betaproteobacteria in the  
170 nitrate-reducing network were greater than in the sulfate-reducing network. Conversely, the  
171 numbers of links associated with nodes assigned to *Anaerolinea* and *Actinobacteria* in the  
172 nitrate-reducing network were smaller than in the sulfate-reducing network.

### 173 **3.2 Keystone nodes in nitrate- and sulfate-reducing networks**

174 We classified nodes into four categories based on their within-module connectivity  
175 ( $K_{within}$ ) and among-module connectivity ( $K_{out}$ ) values: peripherals, articulation nodes, module  
176 hubs, and network hubs (Fig. 2). The nitrate-reducing network had 12 module hub nodes and 7  
177 articulation nodes. The sulfate-reducing network had 15 module hub nodes and 7 articulation  
178 nodes. No network hubs were detected in both of the networks, as no single node had  $K_{within}>3$   
179 and  $K_{out}>1.5$ . The degree of nodes in both networks was not correlated with the relative  
180 abundance of corresponding OTUs (Fig. S3). Most of the module hubs and articulation nodes  
181 had low relative abundance (<0.5%), except module hubs OTU1 (19.8%) in the nitrate-reducing  
182 network, OTU1310 (3.4%) and OTU910 (3.8%) in the sulfate-reducing network, and articulation  
183 node OTU119 (4.3%) in the sulfate-reducing network (Table S1-S2).

### 184 **3.3 Impact of geochemical features and phylogenetic diversity on topological features**

185 We inferred subnetworks for each sample based on OTU-occurrence (Fig. S4-S11). The  
186 geochemical characteristics impacted different topological features in the subnetworks for  
187 nitrate- (Fig. 3a, Fig. S12-S17) and sulfate-reducing microcosms (Fig. 3b, Fig. S18-S22). In the  
188 subnetworks for the nitrate-reducing microcosms, NA concentrations were positively correlated  
189 with mean neighbors, methane concentrations were positively correlated with diameter (Fig. 3a),  
190 nitrate concentrations were positively correlated with mean path length, mean neighbors, and  
191 centralization, dissolved organic carbon (DOC) concentrations were positively correlated with

192 transitivity, and nitrate and nitrite were negatively correlated with transitivity (Fig. 3a). In the  
193 subnetworks for the sulfate-reducing microcosms, methane concentrations were negatively  
194 correlated with vertex number and edge number, the DOC concentrations were negatively  
195 correlated with diameter and mean path length, and sulfate concentrations were negatively  
196 correlated with vertex number, edge number, and mean neighbors (Fig. 3b).

197 Phylogenetic diversity was positively correlated with vertex number, edge number, and  
198 mean degree in subnetworks for both nitrate- (Fig. 3a, Fig. S23) and sulfate-reducing  
199 microcosms (Fig. 3b, Fig. S24), but the correlation coefficient values for sulfate-reducing  
200 microcosms were higher than for nitrate-reducing microcosms. The phylogenetic diversity was  
201 positively correlated with diameter and mean path length in nitrate-reducing microcosms and  
202 was positively correlated with mean neighbors in sulfate-reducing microcosms.

### 203 ***3.4 Modularity in interactome networks***

204 We focused on the modules with at least 5 nodes, which were assemblages with strong  
205 associations in microbial communities. The nitrate-reducing interactome network had 17  
206 modules, 12 of which were connected with links among modules (Fig. 4a). The sulfate-reducing  
207 interactome network had 13 modules, all of which were connected with links among modules  
208 (Fig. 4b). The modularity coefficient of the nitrate-reducing interactome network (0.82) was  
209 greater than that of the sulfate-reducing interactome network (0.78). Given the intense  
210 association among the nodes in the same module, we postulate that nodes in the same module  
211 have potential syntrophic relationships. The taxonomic composition of modules varied within  
212 both networks, suggesting different potential syntrophic associations in different modules (Fig.  
213 4c, Table S1-S2).

214           The number of nodes in the module within each subnetwork varied in both the nitrate-  
215 and sulfate-reducing interactome networks (Fig. 5). In the subnetworks for nitrate-reducing  
216 microcosms, adding AEO caused modules dominated by Actinobacteria (module 2),  
217 Betaproteobacteria (module 10), and Deltaproteobacteria (module 11) to be more prevalent (Fig.  
218 5a-b). Nitrate-amended microcosms with added Merichem NAs had modules dominated by  
219 Actinobacteria (module 3 and 6) (Fig. 5c-d), and microcosms with added clay sediments had  
220 modules dominated by Clostridia (module 1) (Fig. 5a, c). Nitrate-amended microcosms with  
221 added sand sediments had modules dominated by Anaerolineae, Betaproteobacteria, and  
222 Clostridia (Fig. 5b, d). In the subnetworks for sulfate-reducing microcosms, adding AEO caused  
223 the prevalence of modules dominated by Actinobacteria (module 1), Clostridia (module 5),  
224 Bacteroidia (module 10), and Deltaproteobacteria (module 12) (Fig. 5e, f). Sulfate-amended  
225 microcosms with added Merichem NAs had modules dominated by Clostridia and  
226 Deltaproteobacteria (module 7) (Fig. 5g, h), and microcosms with added clay till sediments had a  
227 module dominated by Anaerolineae (module 2) (Fig. 5e, g).

228           We then identified potential syntrophic associations by picking out the generic pairs that  
229 occur more than once in either nitrate- or sulfate-reducing networks. These potential syntrophic  
230 associations might play a critical role in the metabolic processes within these networks. The  
231 genera *Bellilinea*, *Longilinea*, and *Litorilinea* were identified as interior nodes in both networks.  
232 However, the peripheral nodes in the two networks were different in the potential syntrophic  
233 networks for the nitrate- (Fig. 6a) and sulfate-reducing (Fig. 6b) microcosms. We propose that  
234 these interior nodes represent syntrophic microorganisms which initiate the metabolic reactions,  
235 and the peripheral nodes represent microorganisms metabolizing intermediate compounds  
236 coupled with either nitrate reduction or sulfate reduction. In the nitrate-reducing microcosms, the



237 inferred potential syntrophic associations included links from *Bellilinea* to *Jahnella*, from  
238 *Longilinea* to *Aciditerrimonas*, and from *Thauera* to *Rhizobium*. In the sulfate-reducing  
239 microcosms, the inferred potential syntrophic associations included links from *Litorilinea* to  
240 *Desulfomonile*, from *Longilinea* to *Tangfeifania*, from *Olsenella* to *Smithella* and *Desulfobulbus*,  
241 and from *Bellilinea* to *Laceyella*, *Desulfatitalea*, *Rhizobium*, and *Armatimonadetes* gp4.

#### 242 **4. Discussion**

243 This study showed that anaerobic NAs-degrading consortia amended with different  
244 electron acceptors had distinct microbial interactomes. The taxonomic compositions in the  
245 different modules implied that there are different potential syntrophic assemblies. The variation  
246 of module sizes induced by sediment type and NA source indicated that different treatments  
247 affect the potential syntrophic interactions. We identified the same genera initiating the  
248 metabolism of organic compounds in both nitrate- and sulfate-reducing potential syntrophic  
249 networks, but identified different genera involved in metabolizing the intermediate compounds in  
250 each of these networks. The network analysis inferred unique syntrophic associations that have  
251 not been reported previously.

252 Sulfate-reducing networks had more complex connectivity than nitrate-reducing  
253 networks, the latter having a larger subnetwork of shorter diameter with less links, indicating that  
254 syntrophic metabolism may play a greater role in the biodegradation process. The higher  
255 connectivity of the sulfate-reducing networks may indicate the presence of more syntrophic  
256 associations (Fig. 6), and is consistent with the reported prevalence of syntrophic metabolism  
257 under sulfate-reducing environments in wetland sediments [33] and acid sulfate soil associated  
258 with sulfidic sediments [15]. On the other hand, changes in environmental properties are  
259 important drivers of changes in ecological networks in both macro- and microbiological

260 communities [34]. For example, the complexity of the interactome network in the rhizosphere  
261 was induced by higher organic carbon input from plant roots [24]. Similarly, the DOC  
262 concentrations in the sulfate-reducing microcosms were higher than in the nitrate-reducing  
263 microcosms and may have contributed to the increased connectivity and complexity of the  
264 interactome network in the sulfate-reducing microcosms. The correlation between network  
265 topological properties and biogeochemical features (Fig. 3) also supported the impacts of DOC  
266 on the diameter of the sulfate-reducing network.

267 Different association profiles between nitrate- and sulfate-reducing network can be  
268 ascribed to the influence of electron acceptors on microbial compositions and microbial  
269 interactions. More links associated with Alphaproteobacteria and Betaproteobacteria nodes in the  
270 nitrate-reducing network suggested that these taxa play critical roles in a nitrate-reducing  
271 environment. A metatranscriptome study suggested that nitrate reduction was performed  
272 predominantly by Alpha- and Betaproteobacteria in sub-seafloor sediment [35], and a DNA-SIP  
273 analysis indicated that Betaproteobacteria play a role in syntrophic benzene degradation coupled  
274 to nitrate reduction [12]. Sulfate-reducing microcosms fostered associations for Anaerolineae  
275 and Actinobacteria, which often dominate in sulfate-reducing environments [14,15,33].  
276 Anaerolineae are known to be ‘semi-syntrophic’ organisms, degrading carbohydrates  
277 cooperatively with hydrogenotrophic methanogens in methanogenic bioreactors [36].  
278 Actinobacteria have been identified as the primary syntrophs involved in anaerobic benzene  
279 degradation under iron-reducing conditions [13].

280 Within both networks, we identified a number of keystone nodes, including highly-  
281 connected hubs within a module and articulation nodes connecting different modules. The taxa  
282 represented by these keystone nodes may be very important in maintaining network structure.

283 The taxa represented by these keystone nodes may be very important in maintaining network  
284 structure [24]. Synergistetes, a typically syntrophic taxon, was identified as a module hub and  
285 articulation node, confirming the important role of syntrophic metabolism in both nitrate- and  
286 sulfate-reducing environments. The detection of different module hubs in the different cultures  
287 supports the theory that keystone species play critical roles only under certain conditions [37].

288 Identifying modules in networks is important to comprehensively understand microbial  
289 interactions [24]. Network modules represent closely associated functions in metabolic processes  
290 and niche sharing [38], so the higher modularity value in the nitrate-reducing network indicates  
291 close microbial interactions such as syntrophy. Module sizes varied in subnetworks for different  
292 treatments, such as NA components and sediment texture, demonstrating that these treatments  
293 changed the interactions within the microbial communities. The different impacts of those  
294 treatments in nitrate- and sulfate-reducing networks suggest that cultures with different electron  
295 acceptors might have different microbial communities, which are affected differently by the  
296 various treatments. Alternatively, the modules may have responded differently in the two  
297 networks because of functional redundancy of different taxa, where different microbes play the  
298 same functional role in each network [39].

299 The same genera in the class Anaerolineae were inferred to initially metabolize NAs  
300 under both nitrate- and sulfate-reducing conditions. Anaerolineae has been shown to ferment  
301 various sugars and grow better in the presence of H<sub>2</sub>-consuming methanogens, suggesting  
302 syntrophic metabolism [40]. The genera which were identified in the present study to consume  
303 intermediates under nitrate-reducing condition, including *Jahnella*, *Aciditerrimonas*, and  
304 *Rhizobium*, are all identified as denitrifiers [41]. Although *Thauera* and *Rhizobium* have already  
305 been found to co-occur in previous studies [42,43], this study is the first indication of a

306 syntrophic association between *Bellilinea* and *Jahnella*, *Longilinea* and *Aciditerrimonas*, and  
307 *Thauera* and *Rhizobium* under nitrate-reducing conditions. Similarly, most of the genera which  
308 could potentially consume intermediates under sulfate-reducing conditions were identified as  
309 sulfate-reducing bacteria. Co-occurrence of potential syntrophic partners, such as *Olsenella* and  
310 *Smithella* in anaerobic digester sludge [44], *Longilinea* and *Tangfeifania* in a upflow anaerobic  
311 reactor [45], and *Bellilinea* and *Desulfatitalea* in a heavy oil reservoir [43], have been reported in  
312 previous studies using different methods, but this study is the first to identify the syntrophic  
313 interactions between them using network analysis.

314         Currently, our understanding of syntrophic processes is limited due to the few well-  
315 defined co-cultures available [9]. The ‘omics’-based approaches (metagenomics,  
316 metatranscriptomics, and metaproteomics) can be useful to elucidate syntrophic interactions  
317 between uncultured microorganisms [11]. The single amplified genome (SAG) approach can be  
318 used to obtain genetic information on uncultured organisms, and can potentially be applied to  
319 help understand syntrophic processes [21]. Given the extraordinarily high microbial diversity in  
320 environmental samples, both ‘omics’ and SAG approaches need to be used with other processes  
321 to identify the functional substrate degraders existing within the complex environmental  
322 microbial communities [46].

323         The complexity of NAs in the environment prevents the application of SIP in identifying  
324 NAs-degraders [7]. SIP and fluorescent *in situ* hybridization (FISH) are effectively used to label  
325 functional taxa [9]. However, SIP needs suitable <sup>13</sup>C-labeled compounds, which do not exist for  
326 NA. FISH needs known rRNA or functional gene sequences for to design an effective probe, and  
327 is not able to find new syntrophic pathways and relationships. The interactome network provides

328 a new approach for exploring potential syntrophic relationships at the community level  
329 especially for unknown syntrophic relationships and uncultured species.

## 330 **5. Conclusions**

331 This study inferred the microbial interactome networks in anaerobic NAs degrading  
332 microcosms under either nitrate- or sulfate-reducing conditions. The difference in network  
333 complexity and association profiles among taxa in nitrate- and sulfate-reducing microcosms  
334 demonstrates that different electron acceptors lead to distinct microbial relationships. The  
335 relative abundance of keystone nodes was substantially low, highlighting the need to examine  
336 microbial interactions rather than only concerning microbial composition profiles. Network  
337 analysis also revealed that potential syntrophic associations were initial from genera *Bellilinea*,  
338 *Longilinea*, and *Litorilinea* in both interactome networks but interacted with different syntrophic  
339 taxa in the nitrate- and sulfate-reducing microcosms, respectively. These results indicate that  
340 network analysis can be used to reveal an unrecognized dimension of microbial community  
341 variation, and provide a novel approach for exploring potential syntrophic relationships to  
342 enhance petroleum wastes and other persistent organic pollutants biodegradation.

343

## 344 **CRedit authorship contribution statement**

345 **Xiaofei Lv**: Validation, Writing - Original Draft, Visualization. **Bin Ma**: Conceptualization,  
346 Methodology, Supervision. **Korris Lee**: Writing - Review & Editing. **Ania Ulrich**: Supervision,  
347 Funding acquisition.

## 348 **Declaration of Competing Interest**

349 The authors declare that they have no known competing financial interests or personal  
350 relationships that could have appeared to influence the work reported in this paper.

351 **Acknowledgements**

352 This work was jointly supported by the Natural Science and Engineering Research Council of  
353 Canada, and Zhejiang Provincial Natural Science Foundation of China (LD19D060001 and  
354 LQ20C030006). We thank Chonggang Zhang for establishing the initial enrichment.

355 **References**

- 356 [1] J.V. Headley, D.W. McMartin, A Review of the Occurrence and Fate of Naphthenic  
357 Acids in Aquatic Environments, *J. Environ. Sci. Health Part A.* 39 (2004) 1989–2010.  
358 <https://doi.org/10.1081/ESE-120039370>.
- 359 [2] A.A. Holden, S.E. Haque, K.U. Mayer, A.C. Ulrich, Biogeochemical processes  
360 controlling the mobility of major ions and trace metals in aquitard sediments beneath an oil sand  
361 tailing pond: Laboratory studies and reactive transport modeling, *J. Contam. Hydrol.* 151 (2013)  
362 55–67. <https://doi.org/10.1016/j.jconhyd.2013.04.006>.
- 363 [3] E.K. Quagraine, H.G. Peterson, J.V. Headley, In Situ Bioremediation of Naphthenic  
364 Acids Contaminated Tailing Pond Waters in the Athabasca Oil Sands Region—Demonstrated  
365 Field Studies and Plausible Options: A Review, *J. Environ. Sci. Health Part A.* 40 (2005) 685–  
366 722. <https://doi.org/10.1081/ESE-200046649>.
- 367 [4] L.D. Brown, A.C. Ulrich, Oil sands naphthenic acids: A review of properties,  
368 measurement, and treatment, *Chemosphere.* 127 (2015) 276–290.  
369 <https://doi.org/10.1016/j.chemosphere.2015.02.003>.
- 370 [5] A.K.M. Hadwin, L.F. Del Rio, L.J. Pinto, M. Painter, R. Routledge, M.M. Moore,  
371 Microbial communities in wetlands of the Athabasca oil sands: genetic and metabolic  
372 characterization: Microbial communities in wetlands of the Athabasca oil sands, *FEMS*  
373 *Microbiol. Ecol.* 55 (2006) 68–78. <https://doi.org/10.1111/j.1574-6941.2005.00009.x>.

- 374 [6] R.J. Johnson, B.E. Smith, P.A. Sutton, T.J. McGenity, S.J. Rowland, C. Whitby,  
375 Microbial biodegradation of aromatic alkanolic naphthenic acids is affected by the degree of alkyl  
376 side chain branching, *ISME J.* 5 (2011) 486–496. <https://doi.org/10.1038/ismej.2010.146>.
- 377 [7] L.N. Clothier, L.M. Gieg, Anaerobic biodegradation of surrogate naphthenic acids, *Water*  
378 *Res.* 90 (2016) 156–166. <https://doi.org/10.1016/j.watres.2015.12.019>.
- 379 [8] Y. Gunawan, M. Nemati, A. Dalai, Biodegradation of a surrogate naphthenic acid under  
380 denitrifying conditions, *Water Res.* 51 (2014) 11–24.  
381 <https://doi.org/10.1016/j.watres.2013.12.016>.
- 382 [9] L.M. Gieg, S.J. Fowler, C. Berdugo-Clavijo, Syntrophic biodegradation of hydrocarbon  
383 contaminants, *Curr. Opin. Biotechnol.* 27 (2014) 21–29.  
384 <https://doi.org/10.1016/j.copbio.2013.09.002>.
- 385 [10] P. Liu, Q. Qiu, Y. Lu, Syntrophomonadaceae-Affiliated Species as Active Butyrate-  
386 Utilizing Syntrophs in Paddy Field Soil, *Appl. Environ. Microbiol.* 77 (2011) 3884–3887.  
387 <https://doi.org/10.1128/AEM.00190-11>.
- 388 [11] J.R. Sieber, M.J. McInerney, R.P. Gunsalus, Genomic Insights into Syntrophy: The  
389 Paradigm for Anaerobic Metabolic Cooperation, *Annu. Rev. Microbiol.* 66 (2012) 429–452.  
390 <https://doi.org/10.1146/annurev-micro-090110-102844>.
- 391 [12] B.M. van der Zaan, F.T. Saia, A.J.M. Stams, C.M. Plugge, V. de, H. Smidt, A.A.M.  
392 Langenhoff, J. Gerritse, Anaerobic benzene degradation under denitrifying conditions:  
393 Peptococcaceae as dominant benzene degraders and evidence for a syntrophic process, *Environ.*  
394 *Microbiol.* 14 (2012) 1171–1181. <https://doi.org/10.1111/j.1462-2920.2012.02697.x>.

395 [13] U. Kunapuli, T. Lueders, R.U. Meckenstock, The use of stable isotope probing to identify  
396 key iron-reducing microorganisms involved in anaerobic benzene degradation, *ISME J.* 1 (2007)  
397 643–653. <https://doi.org/10.1038/ismej.2007.73>.

398 [14] X. Hong, X. Zhang, B. Liu, Y. Mao, Y. Liu, L. Zhao, Structural differentiation of  
399 bacterial communities in indole-degrading bioreactors under denitrifying and sulfate-reducing  
400 conditions, *Res. Microbiol.* 161 (2010) 687–693.

401 [15] J.L. Stroud, M. Manefield, The microbiology of acid sulfate soils and sulfidic sediments,  
402 *Microbiol. Aust.* 35 (2014) 195–198.

403 [16] S. Herrmann, S. Kleinsteuber, A. Chatzinotas, S. Kuppardt, T. Lueders, H.-H. Richnow,  
404 C. Vogt, Functional characterization of an anaerobic benzene-degrading enrichment culture by  
405 DNA stable isotope probing, *Environ. Microbiol.* 12 (2010) 401–411.

406 [17] L.N. Clothier, L.M. Gieg, Anaerobic biodegradation of surrogate naphthenic acids, *Water*  
407 *Res.* 90 (2016) 156–166. <https://doi.org/10.1016/j.watres.2015.12.019>.

408 [18] T.E. Gibson, A. Bashan, H.-T. Cao, S.T. Weiss, Y.-Y. Liu, On the origins and control of  
409 community types in the human microbiome, *PLoS Comput Biol.* 12 (2016) e1004688.

410 [19] G. Lima-Mendez, K. Faust, N. Henry, J. Decelle, S. Colin, F. Carcillo, S. Chaffron, J.C.  
411 Ignacio-Espinosa, S. Roux, F. Vincent, L. Bittner, Y. Darzi, J. Wang, S. Audic, L. Berline, G.  
412 Bontempi, A.M. Cabello, L. Coppola, F.M. Cornejo-Castillo, F. d’Ovidio, L.D. Meester, I.  
413 Ferrera, M.-J. Garet-Delmas, L. Guidi, E. Lara, S. Pesant, M. Royo-Llonch, G. Salazar, P.  
414 Sánchez, M. Sebastian, C. Souffreau, C. Dimier, M. Picheral, S. Searson, S. Kandels-Lewis, T.O.  
415 Coordinators, G. Gorsky, F. Not, H. Ogata, S. Speich, L. Stemmann, J. Weissenbach, P.  
416 Wincker, S.G. Acinas, S. Sunagawa, P. Bork, M.B. Sullivan, E. Karsenti, C. Bowler, C. de



417 Vargas, J. Raes, Determinants of community structure in the global plankton interactome,  
418 Science. 348 (2015) 1262073. <https://doi.org/10.1126/science.1262073>.

419 [20] S. Freilich, A. Kreimer, I. Meilijson, U. Gophna, R. Sharan, E. Ruppin, The large-scale  
420 organization of the bacterial network of ecological co-occurrence interactions, Nucleic Acids  
421 Res. 38 (2010) 3857–3868. <https://doi.org/10.1093/nar/gkq118>.

422 [21] M.K. Nobu, T. Narihiro, C. Rinke, Y. Kamagata, S.G. Tringe, T. Woyke, W.-T. Liu,  
423 Microbial dark matter ecogenomics reveals complex synergistic networks in a methanogenic  
424 bioreactor, ISME J. 9 (2015) 1710–1722. <https://doi.org/10.1038/ismej.2014.256>.

425 [22] A. Barberán, S.T. Bates, E.O. Casamayor, N. Fierer, Using network analysis to explore  
426 co-occurrence patterns in soil microbial communities, ISME J. 6 (2012) 343–351.  
427 <https://doi.org/10.1038/ismej.2011.119>.

428 [23] B. Ma, H. Wang, M. Dsouza, J. Lou, Y. He, Z. Dai, P.C. Brookes, J. Xu, J.A. Gilbert,  
429 Geographic patterns of co-occurrence network topological features for soil microbiota at  
430 continental scale in eastern China, ISME J. 10 (2016) 1891–1901.  
431 <https://doi.org/10.1038/ismej.2015.261>.

432 [24] S. Shi, E.E. Nuccio, Z.J. Shi, Z. He, J. Zhou, M.K. Firestone, The interconnected  
433 rhizosphere: High network complexity dominates rhizosphere assemblages, Ecol. Lett. 19 (2016)  
434 926–936. <https://doi.org/10.1111/ele.12630>.

435 [25] G. Hwang, T. Dong, Md.S. Islam, Z. Sheng, L.A. Pérez-Estrada, Y. Liu, M. Gamal El-  
436 Din, The impacts of ozonation on oil sands process-affected water biodegradability and biofilm  
437 formation characteristics in bioreactors, Bioresour. Technol. 130 (2013) 269–277.  
438 <https://doi.org/10.1016/j.biortech.2012.12.005>.

439 [26] A.A. Holden, R.B. Donahue, A.C. Ulrich, Geochemical interactions between process-  
440 affected water from oil sands tailings ponds and North Alberta surficial sediments, *J. Contam.*  
441 *Hydrol.* 119 (2011) 55–68. <https://doi.org/10.1016/j.jconhyd.2010.09.008>.

442 [27] N. Fierer, R.B. Jackson, The diversity and biogeography of soil bacterial communities,  
443 *Proc. Natl. Acad. Sci. U. S. A.* 103 (2006) 626–631.

444 [28] X. Lv, B. Ma, D. Cologgi, K. Lee, A. Ulrich, Naphthenic Acid Anaerobic Biodegrading  
445 Consortia Enriched from Pristine Sediments Underlying Oil Sands Tailings Ponds, *J. Hazard.*  
446 *Mater.* (2020) 122546. <https://doi.org/10.1016/j.jhazmat.2020.122546>.

447 [29] D. Albanese, M. Filosi, R. Visintainer, S. Riccadonna, G. Jurman, C. Furlanello, minerva  
448 and minepy: a C engine for the MINE suite and its R, Python and MATLAB wrappers,  
449 *Bioinformatics.* 29 (2013) 407–408.

450 [30] S. Feizi, D. Marbach, M. Médard, M. Kellis, Network deconvolution as a general method  
451 to distinguish direct dependencies in networks, *Nat. Biotechnol.* 31 (2013) 726–733.

452 [31] F. Luo, J. Zhong, Y. Yang, R.H. Scheuermann, J. Zhou, Application of random matrix  
453 theory to biological networks, *Phys. Lett. A.* 357 (2006) 420–423.

454 [32] G. Csardi, T. Nepusz, The igraph software package for complex network research,  
455 *InterJournal Complex Syst.* 1695 (2006) 1–9.

456 [33] P. Dalcin Martins, D.W. Hoyt, S. Bansal, C.T. Mills, M. Tfaily, B.A. Tangen, R.G.  
457 Finocchiaro, M.D. Johnston, B.C. McAdams, M.J. Solensky, G.J. Smith, Y.-P. Chin, M.J.  
458 Wilkins, Abundant carbon substrates drive extremely high sulfate reduction rates and methane  
459 fluxes in Prairie Pothole Wetlands, *Glob. Change Biol.* (2017) n/a-n/a.  
460 <https://doi.org/10.1111/gcb.13633>.

461 [34] B. Allen, G. Lippner, Y.-T. Chen, B. Fotouhi, N. Momeni, S.-T. Yau, M.A. Nowak,  
462 Evolutionary dynamics on any population structure, *Nature*. 544 (2017) 227–230.  
463 <https://doi.org/10.1038/nature21723>.

464 [35] W.D. Orsi, V.P. Edgcomb, G.D. Christman, J.F. Biddle, Gene expression in the deep  
465 biosphere, *Nature*. 499 (2013) 205–208. <https://doi.org/10.1038/nature12230>.

466 [36] T. Narihiro, T. Terada, A. Ohashi, Y. Kamagata, K. Nakamura, Y. Sekiguchi,  
467 Quantitative detection of previously characterized syntrophic bacteria in anaerobic wastewater  
468 treatment systems by sequence-specific rRNA cleavage method, *Water Res.* 46 (2012) 2167–  
469 2175. <https://doi.org/10.1016/j.watres.2012.01.034>.

470 [37] M.E. Power, D. Tilman, J.A. Estes, B.A. Menge, W.J. Bond, L.S. Mills, G. Daily, J.C.  
471 Castilla, J. Lubchenco, R.T. Paine, Challenges in the Quest for Keystones Identifying keystone  
472 species is difficult—but essential to understanding how loss of species will affect ecosystems,  
473 *BioScience*. 46 (1996) 609–620. <https://doi.org/10.2307/1312990>.

474 [38] K. Faust, J. Raes, Microbial interactions: from networks to models, *Nat. Rev. Microbiol.*  
475 10 (2012) 538–550. <https://doi.org/10.1038/nrmicro2832>.

476 [39] S.D. Allison, J.B. Martiny, Resistance, resilience, and redundancy in microbial  
477 communities, *Proc. Natl. Acad. Sci.* 105 (2008) 11512–11519.

478 [40] T. Yamada, H. Imachi, A. Ohashi, H. Harada, S. Hanada, Y. Kamagata, Y. Sekiguchi,  
479 *Bellilinea caldifistulae* gen. nov., sp. nov. and *Longilinea arvoryzae* gen. nov., sp. nov., strictly  
480 anaerobic, filamentous bacteria of the phylum Chloroflexi isolated from methanogenic  
481 propionate-degrading consortia, *Int. J. Syst. Evol. Microbiol.* 57 (2007) 2299–2306.  
482 <https://doi.org/10.1099/ijs.0.65098-0>.

483 [41] L. Chu, J. Wang, Denitrification performance and biofilm characteristics using  
484 biodegradable polymers PCL as carriers and carbon source, *Chemosphere*. 91 (2013) 1310–1316.  
485 <https://doi.org/10.1016/j.chemosphere.2013.02.064>.

486 [42] P. Gao, H. Tian, Y. Wang, Y. Li, Y. Li, J. Xie, B. Zeng, J. Zhou, G. Li, T. Ma, Spatial  
487 isolation and environmental factors drive distinct bacterial and archaeal communities in different  
488 types of petroleum reservoirs in China, *Sci. Rep.* 6 (2016).  
489 <https://www.ncbi.nlm.nih.gov/pmc/articles/PMC4738313/>.

490 [43] L. Wang, Y. Nie, Y.-Q. Tang, X.-M. Song, K. Cao, L.-Z. Sun, Z.-J. Wang, X.-L. Wu,  
491 Diverse bacteria with lignin degrading potentials isolated from two ranks of coal, *Front.*  
492 *Microbiol.* 7 (2016). <https://www.ncbi.nlm.nih.gov/pmc/articles/PMC5016517/>.

493 [44] T. Ito, K. Yoshiguchi, H.D. Ariesyady, S. Okabe, Identification and quantification of key  
494 microbial trophic groups of methanogenic glucose degradation in an anaerobic digester sludge,  
495 *Bioresour. Technol.* 123 (2012) 599–607.

496 [45] P. Antwi, J. Li, P.O. Boadi, J. Meng, F. Koblah Quashie, X. Wang, N. Ren, G. Buelna,  
497 Efficiency of an upflow anaerobic sludge blanket reactor treating potato starch processing  
498 wastewater and related process kinetics, functional microbial community and sludge  
499 morphology, *Bioresour. Technol.* 239 (2017) 105–116.  
500 <https://doi.org/10.1016/j.biortech.2017.04.124>.

501 [46] Ö. Eyice, M. Namura, Y. Chen, A. Mead, S. Samavedam, H. Schäfer, SIP metagenomics  
502 identifies uncultivated Methylophilaceae as dimethylsulphide degrading bacteria in soil and lake  
503 sediment, *ISME J.* 9 (2015) 2336–2348. <https://doi.org/10.1038/ismej.2015.37>.

504

505 **Figure legends**

506 Figure 1. Interactome networks for (a) nitrate-reducing microcosms and (b) sulfate-  
507 reducing microcosms; The associations among classes in the network for (c) nitrate-reducing  
508 microcosms and (d) sulfate-reducing microcosms.

509 Figure 2. The keystone nodes in the networks for nitrate- and sulfate-reducing  
510 microcosms. Module hubs represent nodes with  $K_{\text{within}} > 3$  and articulation nodes represent nodes  
511 with  $K_{\text{out}} > 1.5$ .

512 Figure 3. Correlation matrices between network topological properties and geochemical  
513 properties in (a) nitrate- and (b) sulfate-reducing microcosms. The color and size of circles  
514 represent values of the Pearson correlation coefficient. The crosses represent non-significant  
515 correlations ( $p > 0.05$ ). PD=phylogenetic diversity; DOC=dissolved organic matters.

516 Figure 4. The modules of interactome networks for (a) nitrate- and (b) sulfate-reducing  
517 microcosms and (c) the taxonomic compositions of modules. The numbers indicate the specific  
518 module number.

519 Figure 5. The sizes of modules in subnetworks for (a-d) nitrate- and (e-h) sulfate-  
520 reducing microcosms with (a-b, e-f) AEO or (c-d, g-h) Merichem NAs, and (a, c, e, g) clay or (b,  
521 d, f, h) sandy sediments.

522 Figure 6. Potentially syntrophic associations in (a) nitrate- and (b) sulfate-reducing  
523 microcosms. The links represent generic pair associations occurring more than one time in  
524 nitrate- or sulfate-reducing networks. Red lines represent potential syntrophic associations  
525 between interior and peripheral nodes.

526

527

528 **Tables**

529 **Table 1.** Topological properties for the interactome networks for nitrate- and sulfate-  
530 reducing microcosms and their corresponding random Erdos-Renyi networks

Networks	Node number	Link number	Mean link number	Diameter	Mean path length	Mean neighbor number	Centrality	Transitivity
Nitrate-reducing network	239	226	0.95	19.0	8.38	2.21	0.076	0.14
Random network 1	239	226	0.95	22.0	9.81	2.42	0.100	0.00
Sulfate-reducing network	238	212	0.89	15.2	7.58	2.17	0.129	0.15
Random network 2	238	212	0.89	24.0	8.88	2.34	0.104	0.01

531

532 **Associated content**

533 Supporting Information.

534 The following files are available free of charge.

535 Figure S1-S24 (PDF).

536 **Table S1. The module and taxon of nodes in the interactome network for nitrate-reducing**  
537 **microcosms (CSV).**

538 **Table S2. The module and taxon of nodes in the interactome network for sulfate-reducing**  
539 **microcosms (CSV).**

540 **Author contributions**

541 The manuscript was written through contributions of all authors. All authors have given  
542 approval to the final version of the manuscript.

543 **Funding sources**

544           This work was jointly supported by the Natural Science and Engineering Research  
545 Council of Canada, and the Zhejiang Provincial Natural Science Foundation of China  
546 (LD19D060001 and LQ20C030006).

**CRedit authorship contribution statement**

**Xiaofei Lv**: Validation, Writing - Original Draft, Visualization. **Bin Ma**:  
Conceptualization, Methodology, Supervision. **Korris Lee**: Writing - Review &  
Editing. **Ania Ulrich**: Supervision, Funding acquisition.



**Declaration of interests**

The authors declare that they have no known competing financial interests or personal relationships that could have appeared to influence the work reported in this paper.

The authors declare the following financial interests/personal relationships which may be considered as potential competing interests:

Figure1  
[Click here to download high resolution image](#)

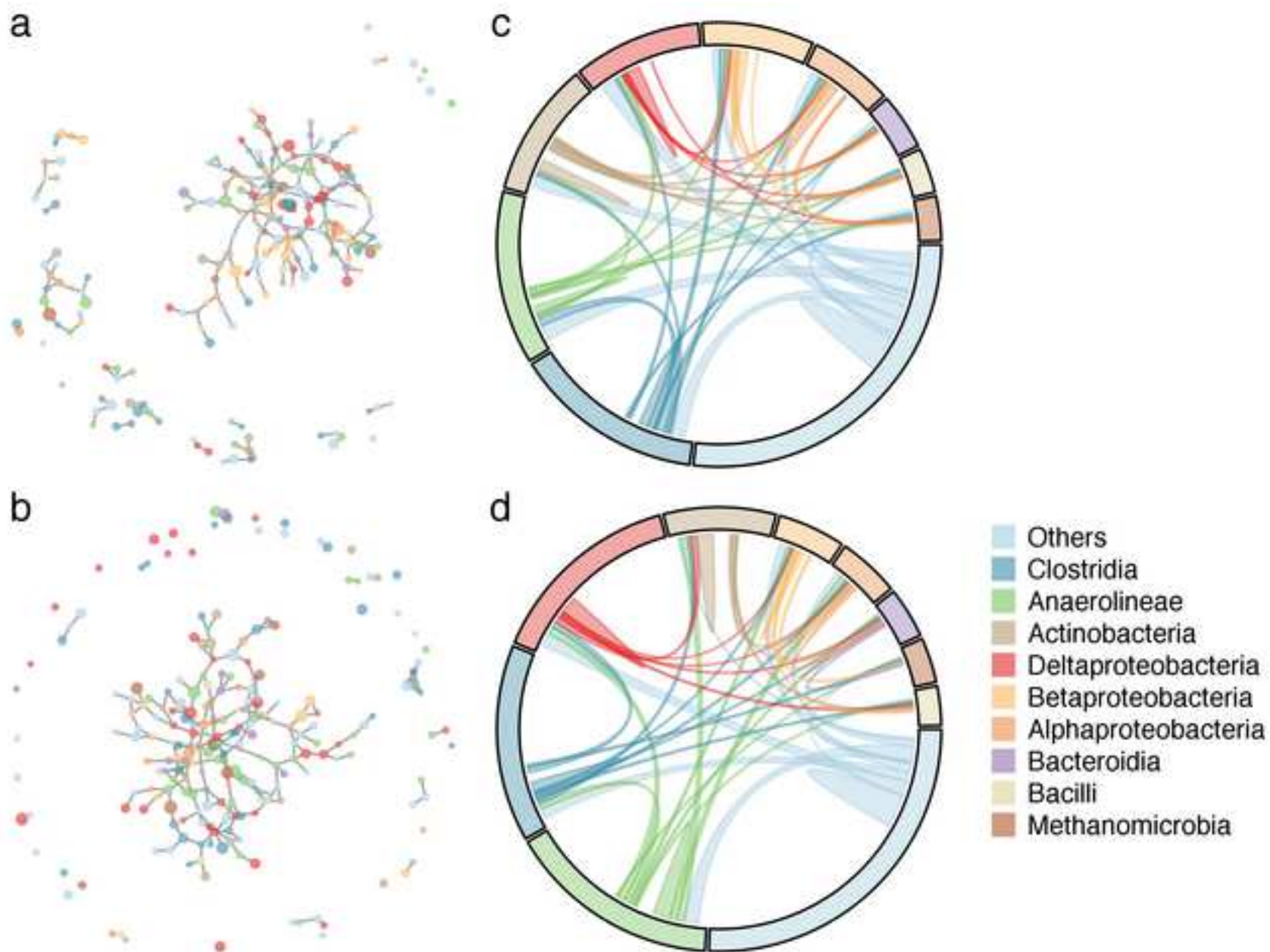


Figure2

[Click here to download high resolution image](#)

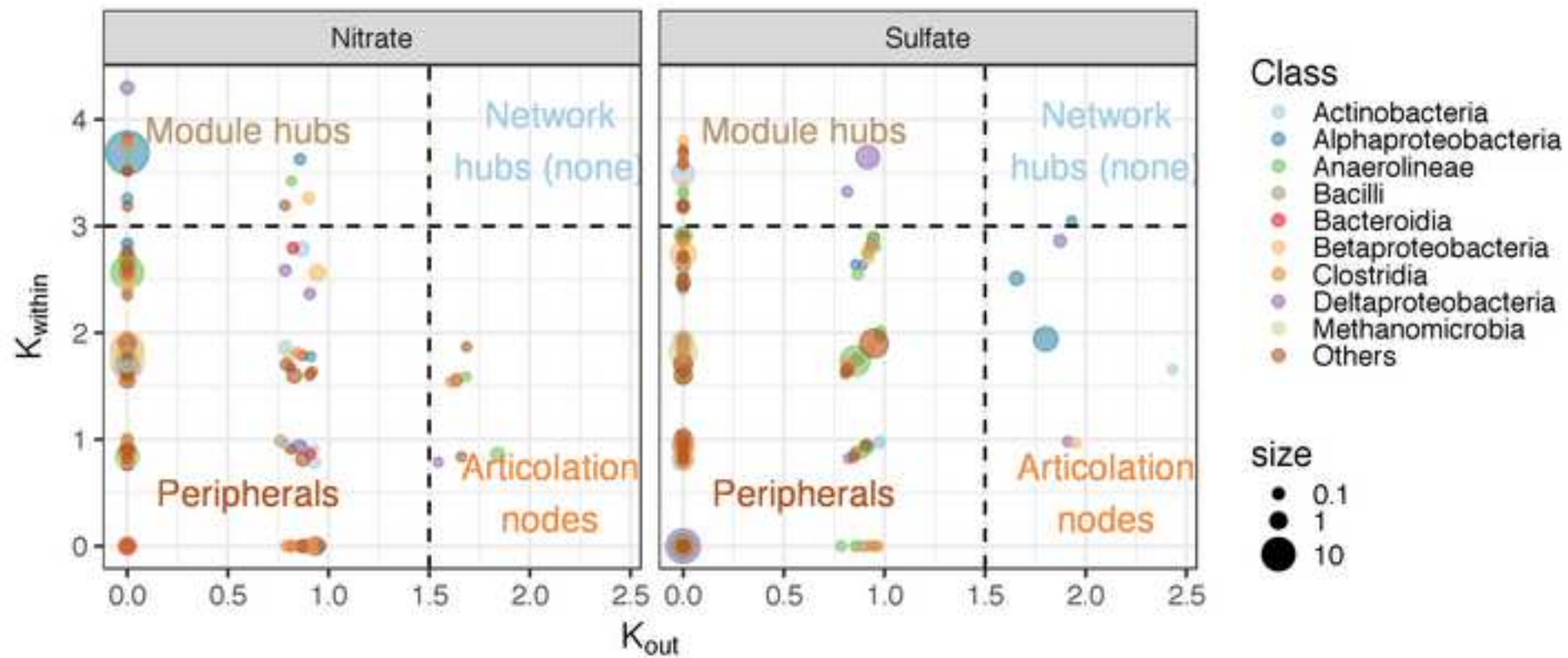


Figure3

[Click here to download Figure3\\_corplot.eps](#)

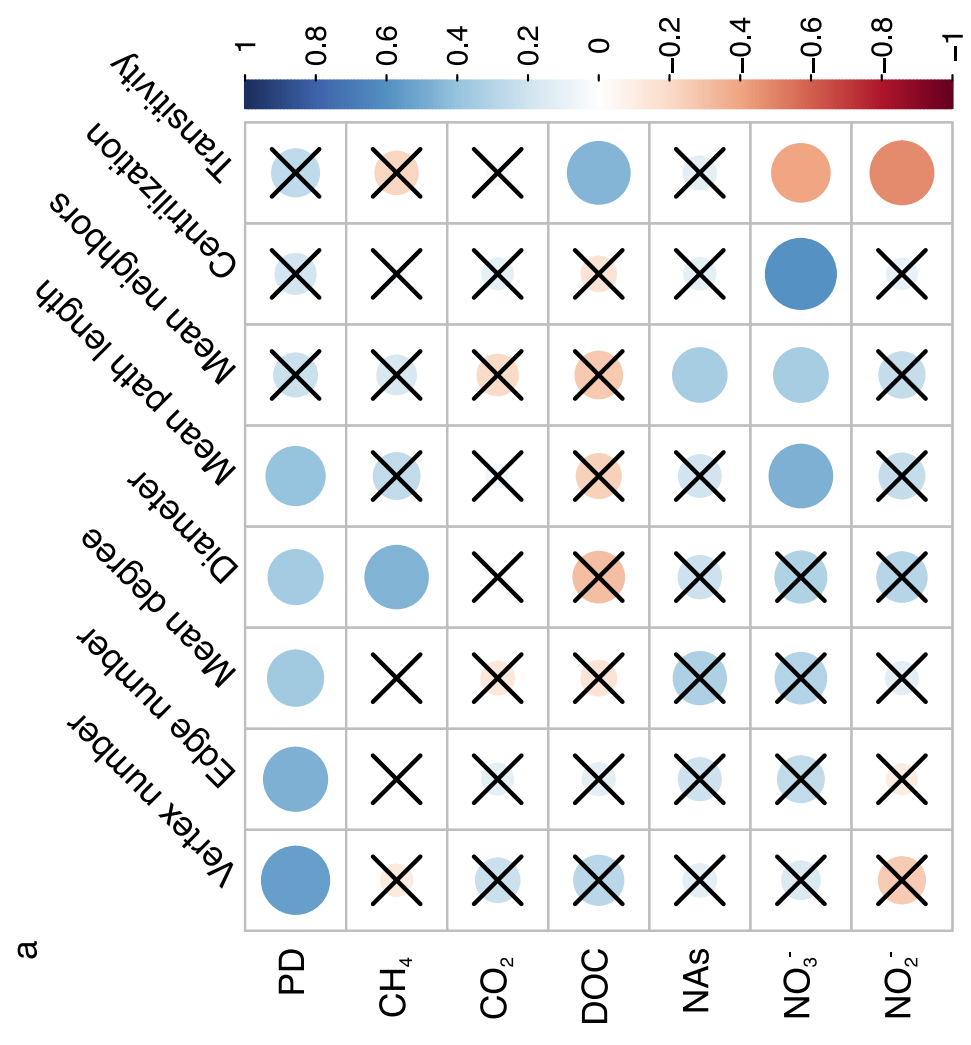
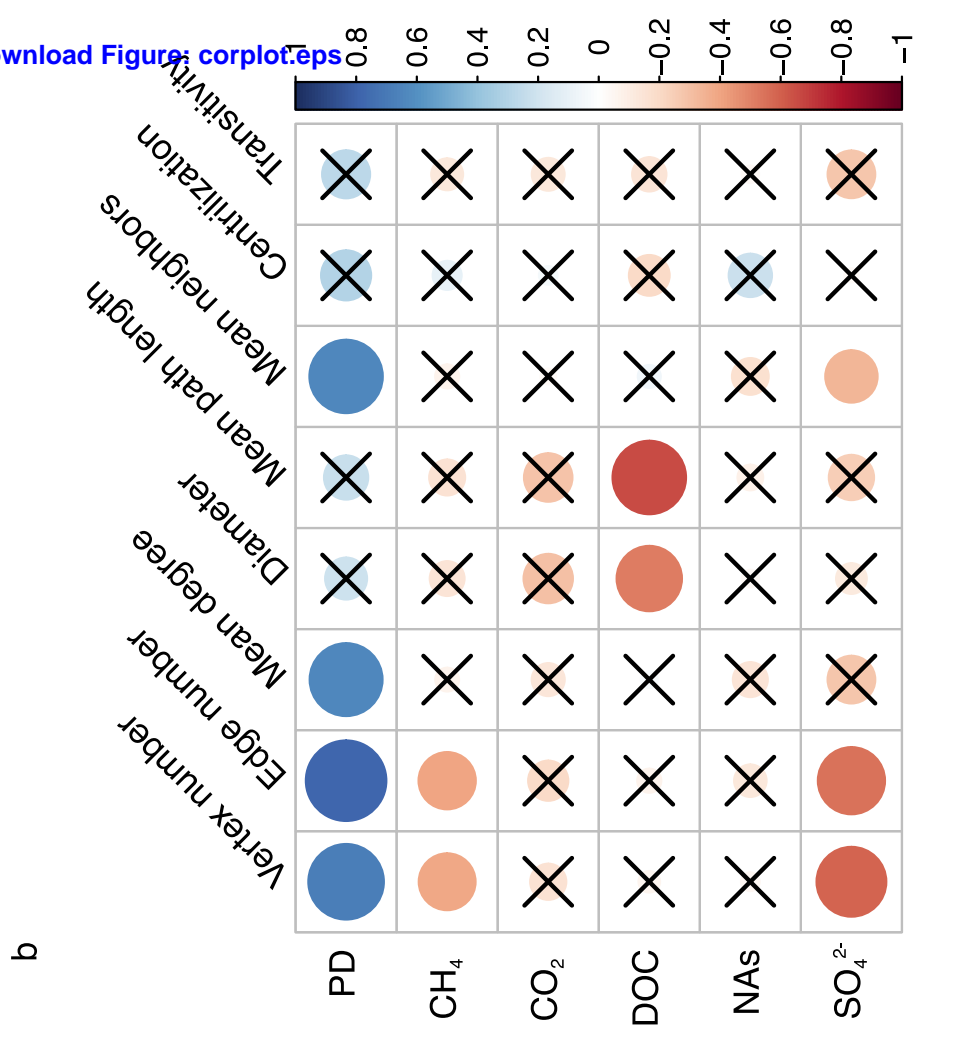


Figure4

[Click here to download high resolution image](#)

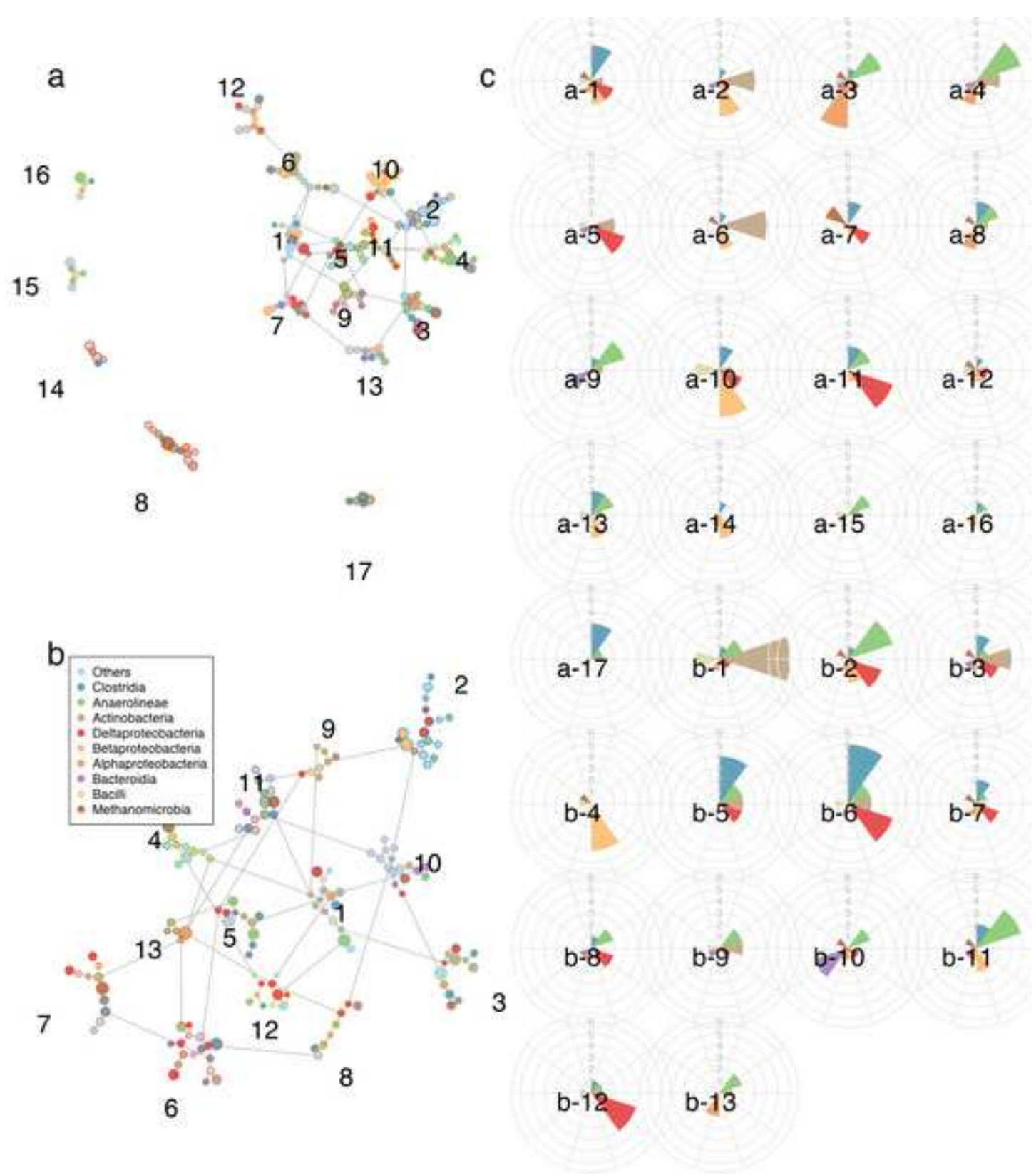


Figure5

[Click here to download high resolution image](#)

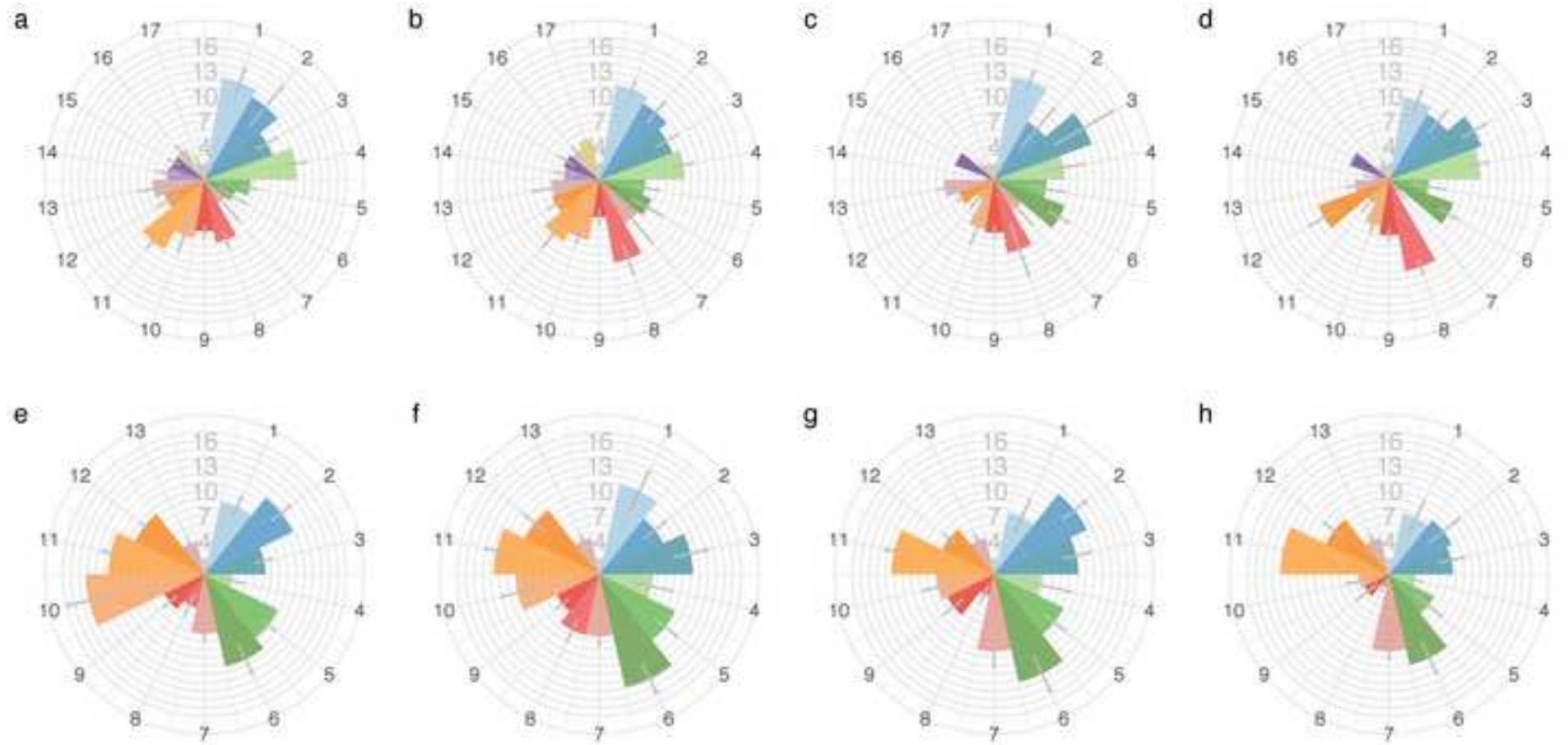
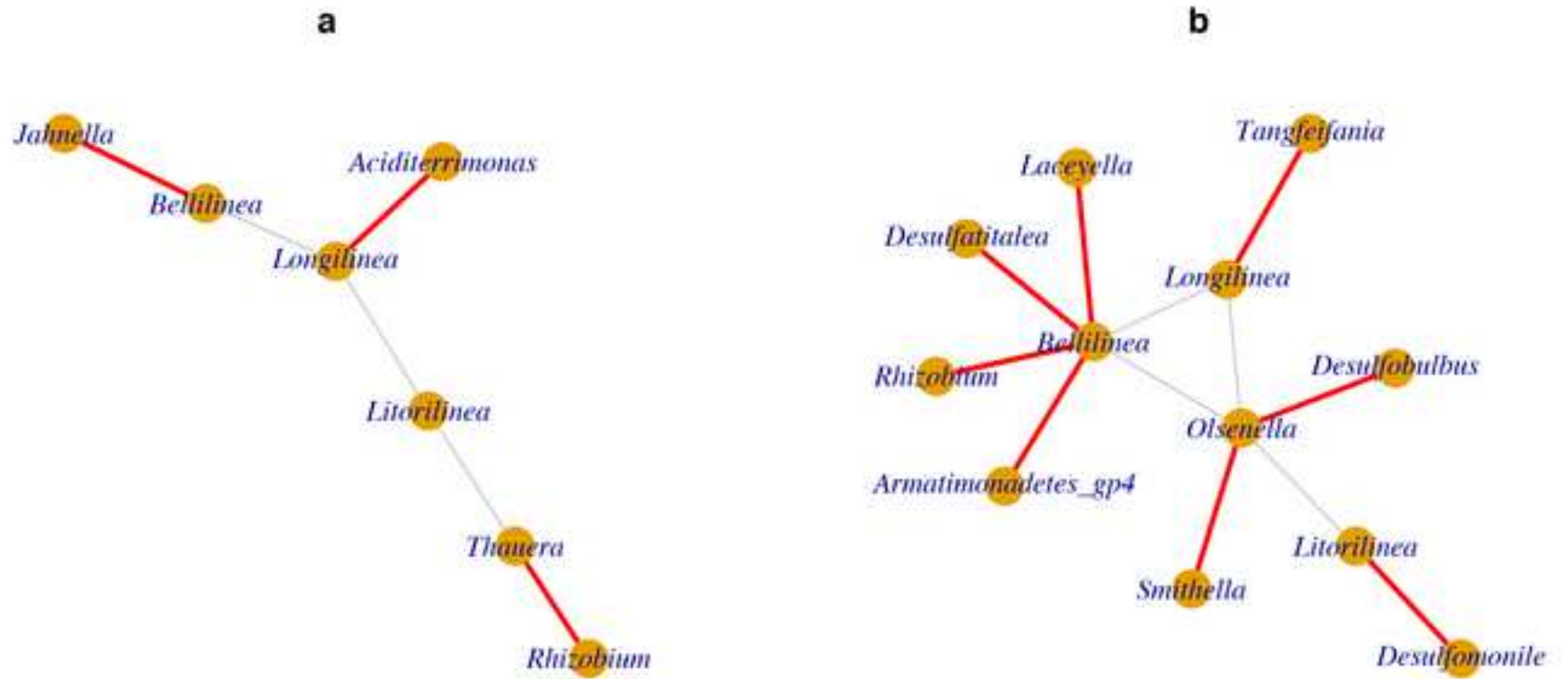


Figure6  
[Click here to download high resolution image](#)



**Supplementary Material**

[Click here to download Supplementary Material: Supporting materials\\_V2.docx](#)



**Supplementary Material**

[Click here to download Supplementary Material: Table\\_S1.csv](#)

**Supplementary Material**

[Click here to download Supplementary Material: Table\\_S2.csv](#)